Published in final edited form as:
Magn Reson Imaging. 2013 July ; 31(6): 1006–1011. doi:10.1016/j.mri.2013.03.001.

Novel S-Gal® analogs as ^{1}H MRI reporters for in vivo detection of β-galactosidase

Praveen K. Gulaka[a,1], **Jian-Xin Yu**[b], **Li Liu**[b], **Ralph P. Mason**[a,b], and **Vikram D. Kodibagkar**[a,b,c,*]

Vikram D. Kodibagkar: vikram.kodibagkar@asu.edu

[a]Joint program in Biomedical Engineering, University of Texas Southwestern Medical Center, Dallas, TX, 75390 and University of Texas at Arlington, Arlington, TX 76019, USA

[b]Department of Radiology, University of Texas Southwestern Medical Center, Dallas, TX, 75390, USA

[c]School of Biological and Health Systems Engineering, Arizona State University, Phoenix, AZ, 85287, USA

Abstract

The quantitative assessment of gene expression and related enzyme activity *in vivo* could be important for the characterization of gene altering diseases and therapy. The development of imaging techniques, based on specific reporter molecules may enable routine non-invasive assessment of enzyme activity and gene expression *in vivo*. We recently reported the use of commercially available S-Gal® as a β-galactosidase reporter for ^{1}HMRI, and the synthesis of several S-Gal® analogs with enhanced response to β-galactosidase activity. We have now compared these analogs *in vitro* and have identified the optimal analog, C3-GD, based on strong T_1 and T_2 response to enzyme presence (ΔR_1 and $\Delta R_2 \sim 1.8$ times S-Gal®). Moreover, application is demonstrated *in vivo* in human breast tumor xenografts. MRI studies in MCF7-*lacZ* tumors implanted subcutaneously in athymic nude mice (n = 6), showed significant reduction in T_1 and T_2 values (each ~ 13%) 2 h after intratumoral injection of C3-GD, whereas the MCF7 (wild type) tumors showed slight increase. Thus, C3-GD successfully detects β-galactosidase activity *in vivo* and shows promise as a *lacZ* gene ^{1}HMR reporter molecule.

Keywords

β-galactosidase; ^{1}H MRI; T_1; T_2; Signal enhancement; Fe-chelation; *lacZ*; Gene reporters

1. Introduction

One of the major challenges in the field of gene therapy has been the lack of methods to quantitatively assess the success of gene transfection and the longevity of gene expression [1]. Reporter genes are typically used to assess regulation and transfection of genes in biological pathways. Popular reporter genes are those that generate β-galactosidase (β-gal), β-glucuronidase, firefly luciferase, fluorescent proteins (*e.g.*, green fluorescent protein), transferrin and ferritin [1–3]. Historically, the *lacZ* gene encoding β-gal has been the most

*Corresponding author. School of Biological and Health Systems Engineering, Arizona State University, Phoenix, AZ, 85287–9709, USA. Tel.: +1 480 965 4635; fax: +1 480 727 7624.

[1]Currently with Samsung Electronics, Suwon, South Korea.

extensively used reporter with applications ranging from basic science to translational and clinical trials for assaying protein expression and interactions [4,5].

There are various commercially available reagents (substrates) in regular use to detect β-gal expression *in vitro* by colorimetric stains and assays, such as nitrophenyl-β-D-galactopyranoside (generates yellow color) [6], 4-chloro-3-bromoindole-galactose (X-Gal®, generates a blue stain) [7] and 3,4-cyclohexenoesculetin β-D-galactopyranoside (S-Gal® - generates a black stain) [8]. The β-gal expression is also associated with cellular senescence [9] and X-Gal® has been used to assay senescence-associated β-gal *in vitro* and *ex vivo* [10].

In recent years, development of novel reporter molecules and techniques for non-invasive *in vivo* detection of β-gal activity, as a marker of *lacZ* transgene expression, has been reported including optical [11–13], photoacoustic [14], radionuclide [15,16] and MR imaging (^{1}H [17–19] and/or ^{19} F [19–24]) methods. In a recent study, we demonstrated the ability to detect β-gal activity in *lacZ*-transfected breast cancer cells (MCF7) *in vitro* and *in vivo* using the commercially available S-Gal® by ^{1}H MRI [25]. We also demonstrated the synthesis of several S-Gal® analogs for improved response to β-gal activity [26]. In both cases, β-gal cleaves the substrate molecule at the C-O bond between β-D-galactopyranoside and aglycone, to release the aglycone, which forms a paramagnetic chelate in the presence of Fe^{3+} generating T1/T2/T_2^*-weighted ^{1}H MRI contrast. Fig. 1 illustrates the mechanism for ^{1}H-MRI detection of β-gal activity, using C3-GD as a model reporter. In the present study, we have compared the S-Gal® analogs *in vitro* and shown application of the lead agent for detection of β-galactosidase activity in human breast tumor xenografts.

2. Materials and methods

2.1. General

3,4-Cyclohexenoesculetin β-D-galactopyranoside (S-Gal® sodium salt), and ferric ammonium citrate (FAC) were purchased from Sigma-Aldrich (St. Louis, MO). Monogalactopryanosides 7-*O*-(β-D-galactopyranosyl)-8-hydroxy-3, 4-cyclohexenocoumarin (C1-MGD), 7-*O*-(β-D-galactopyranosyl)-8-hydroxy-4-methylcoumarin (C2-MGD), 7-*O*-(β-D-galactopyranosyl)-6-hydroxy-4-methylcoumarin (C3-MGD), 7-*O*-(β-D-galactopyranosyl)-8-hydroxy-6-methoxycoumarin (C4-MGD) and digalactopryanosides 7,8-di-*O*-(β-D-galactopyranosyl)-3, 4-cyclohexenocoumarin (C1-GD), 7,8-di-*O*-(β-D-galactopyranosyl)-4-methylcoumarin (C2-GD), 6,7-di-*O*-(β-D-galactopyranosyl)-4-methylcoumarin (C3-GD), 7,8-di-*O*-(β-D-galactopyranosyl)-6-methoxycoumarin (C4-GD) (Fig. 2) were synthesized by us as described previously [26]. All MR studies were performed on a Varian INOVA 4.7 T horizontal-bore MR system (200 MHz for ^{1}H) equipped with actively shielded gradients. T_1 mapping was performed using a spin echo sequence with TE = 12 ms and varying TR (0.2–6 s), while T_2 mapping was performed using a spin echo sequence with varying TE (12–200 ms) and TR = 6 s.

2.2. Detection of β-gal activity in vitro

For *in vitro* measurements, each reporter molecule solution (15 mM in de-ionized water, 40 μL) was mixed with FAC (5 mM, 40 μL) in 2% agar solution with or without β-gal (5 units, E801A, Sigma-Aldrich, St. Louis, MO) and placed in a 4 × 4 cut section of a 96 well plate. The prepared phantom was placed on a heating block maintained at 37 °C for 30 mins for the enzymatic reaction to stabilize. T_1 and T_2 maps of the phantom were acquired using a 3 cm solenoid coil (home-built) at 37 °C. MRI parameters: FOV 40 mm × 40 mm, matrix size 128 × 128, slice thickness 1 mm.

2.3. In vivo detection of β-gal activity in MCF7 and MCF7-lacZ tumors

All *in vivo* studies were performed with approval from the UT Southwestern Medical Center Animal Care and Use Committee. MCF7 (wild-type 1.5×10^6) and MCF7-*lacZ* (2×10^6) cells were implanted subcutaneously in the thighs of athymic nude mice (N = 6) on contralateral sides. MRI studies were performed when the tumor size reached 0.75 cm^3. Mice were anesthetized with 1.5% isoflurane in air and placed in a Litzcage volume coil (Doty Scientific Inc, Columbia, SC) for MRI. Animal body temperature was maintained at 37 °C using a circulating warm water pad. Baseline (pre-injection) T_1 and T_2 maps of tumor containing slices were acquired using MRI parameters: FOV 100 mm × 50 mm, matrix size 256 × 128, slice thickness 1 mm, 13 slices. Following baseline imaging, the mouse was removed from the scanner and 25 μL of a solution containing 15 mM C3-GD and 5 mM FAC in water was injected intra-tumorally in a fan pattern in a sagittal plane using a fine 32G Hamilton® needle into each tumor. After repositioning the mouse carefully, T_1 and T_2 maps were acquired 1 and 2 hours post injection. Multiple slices were acquired and those with injected contrast agent were identified based on the T_2- and T_1-weighted images (to delineate tumor boundary and locate the injected Fe^{3+} ions, respectively) for analysis. Tumor voxels from the injected slice of all animals were pooled with respect to imaging time point (baseline, 1 h and 2 h post injection) and statistical analysis with one-way ANOVA followed by Bonferroni's multiple comparison test was performed using GraphPad Prism (GraphPad Software Inc., La Jolla, CA).

2.4. Histology

Following MRI, the tumors were excised and fixed in 4% formalin. These tumor sections were embedded in paraffin and then cut into 5 μm-thick sections. These sections were further stained with 4-chloro-3-bromoindole-galactoside (X-Gal®) and counter stained by nuclear fast red to reveal β-gal activity and nuclear locations respectively.

3. Results

3.1. Comparison of reporter molecules in vitro

T_1 and T_2 maps of the reporter molecules together with FAC in agar gel phantoms showed varying contrast in the presence of 5 units β-gal (Fig. 3). The largest responses in T_1 were observed for C3-GD, C2-MGD and C3-MGD with decreases of 1.12 s, 1.24 s, and 1.17 s, respectively, which is greater than 1.03 s observed using S-Gal® (Table 1). Similarly, C3-GD and C3-MGD showed a decrease in T_2 of 45 ms and 95 ms respectively, which is significantly higher than 23 ms observed using S-Gal® (Table 1). These values correspond to ΔR_1 and ΔR_2 about 1.8 times greater than S-Gal® for C3-GD and $\Delta R_1 \sim 2.8$ and $\Delta R_2 \sim 6.5$ times S-Gal® for C3-MGD. C3-GD was used for further *in vivo* studies due to better water solubility than C3-MGD.

3.2. Evaluation of reporter molecule C3-GD in vivo

T_1 and T_2 maps of athymic nude mice bearing wild-type (WT) and *lacZ*-transfected MCF7 tumors before and after the injection of C3-GD (15 mM) + FAC (5 mM) solution (25 μL vol.) are shown in Fig. 4. T_1-weighted images showed small hyper-intensities, which were better perceived from the decrease in T_1 values, as seen in the T_1 maps of representative tumor slices (Fig. 3a). There was a small, but significant, difference between mean baseline T_1 (1.84 ± 0.28 s; WT (n = 6) vs. 1.88 ± 0.22 s; *lacZ* (n = 6); $p < 0.0001$; unpaired t-test) of the two tumor types (Table 2). Following injection of reporter molecule solution (C3-GD + FAC), T_1 decreased significantly in WT tumors ($T_1 = 1.72 \pm 0.29$ s, $p < 0.0001$) after 1 h, but recovered back by the end of 2 h ($T_1 = 1.97 \pm 0.35$ s, $p < 0.0001$) to exceed pre-injection values. In *lacZ* tumors, T_1 decreased significantly by the end of 1 h ($T_1 = 1.69 \pm 0.33$ s, $p < 0.0001$) and showed continued decrease at 2 h ($T_1 = 1.63 \pm 0.25$ s, $p < 0.0001$).

Analysis of the same ROIs (as in T_1 analysis) on T_2 maps showed large decrease in T_2 for MCF7-*lacZ* tumors when compared to baseline (Fig. 4b). There was a significant difference in the baseline T_2 values of WT and *lacZ* transfected tumors ($T_2 = 56 \pm 16$ ms (WT) vs. $T_2 = 51 \pm 8$ ms (*lacZ*); $p < 0.0001$; unpaired t-test). Following administration of the solution of C3-GD + FAC, T_2 decreased significantly in WT tumors ($T_2 = 51 \pm 16$ ms; $p < 0.0001$) at 1 h, but returned back to baseline value ($T_2 = 57 \pm 18$ ms; $p > 0.05$) at 2 h (Table 2). In *lacZ* tumors, T_2 decreased significantly by the end of 1 h ($T_2 = 44 \pm 10$, $p < 0.0001$) and remained unchanged at 2 h ($T_2 = 44 \pm 9$, $p < 0.0001$). The X-gal and nuclear fast staining of tumor slices (Fig. 4) obtained following the MRI showed an intense blue stain representing β-gal activity only in the MCF7-*lacZ* tumor, and not in the MCF7 wild-type tumor (Fig. 4c).

4. Discussion

We have demonstrated the relative relaxation response of various S-Gal® analogs to β-galactosidase. ^{1}H MR showed both T_1 and T_2 response *in vitro* and the lead agent was examined *in vivo*. The mono- and di-galactopyranosides showed differential enhancements in response to β-gal in the presence of ferric ions (Fe^{3+} from FAC). The aglycone products readily form paramagnetic iron chelates causing pronounced T_1 and T_2 shortening in MR images. The mono-galactopyranosides always showed better T_1 and T_2 contrast when compared to their associated di-galactopyranosides: *e.g.*, C2-MGD and C3-MGD showed greater T_1 & T_2 shortening than C2-GD and C3-GD, respectively (Fig. 2). This can be attributed to the need for two reactions on the di-galactopyranoside before liberating the aglycone to form the iron chelate. The mono and di-galactopyranosides display a variety of hydrolytic rate constants all of which lead to reaction completion times that are greater than the 30 min incubation time used here (even after accounting for the higher enzyme amount used in [26]). Thus, differences between various analogs may reflect differences in product generation at the 30 min time point apart from the relaxivities of the chelation complexes. C3-MGD and C3-GD both demonstrated pronounced T_1 and T_2 shortening in the presence of 5 units of β-gal, but given its better water solubility, C3-GD was used for *in vivo* studies. Our goal in this study was to compare the various synthesized gene reporter molecules and identify lead candidates *in vitro* followed by *in vivo* testing of detectability of reporter activity. With that in mind, the intra-tumoral injection route was preferred over i.v. delivery to ensure consistent deposition of equal amount of the agent in *lacZ* transfected and control tumors. In comparison, an i.v. delivery would have resulted in heterogeneous deposition of the agent due to variations in vasculature and confounded the testing by the inability to distinguish between poor delivery and poor *in vivo* activity. We do note that solubility was not an issue for intratumoral delivery, but it could be important for potential systemic delivery applications in the future. At the concentrations used for direct intra-tumoral injections in this study, either agent could have been used and given the higher contrast effect and lower solubility, we can expect better performance of C3-MGD for applications that permit intra-tissue injection of the reporter probes. Given that the chelation complex is identical for C3-MGD and C3-GD, other practical concerns such as hydrolytic rates, cellular uptake and retention may dominate the effective observed contrast *in vivo*.

Following intra-tumoral injection of the C3-GD/FAC combination in wild type tumors, we observed a decrease in T_1 and T_2 from baseline to 1 h followed by return to baseline values by 2 h. This initial decrease in T_1 and T_2 values can be attributed to the free ferric ions, which are eventually cleared. In the *lacZ* expressing tumors, paramagnetic complexes are formed due to the chelation of ferric ions by the β-gal-cleaved aglycone molecules. This causes a shortening of T_1 and T_2 when compared to baseline (pre-injection) measurements. Catechol moieties exhibit a high affinity for Fe^{3+} and the complex is expected to stabilize the ferric state preventing other changes under biological conditions [27,28]. The aglycone-Fe^{3+} complex is poorly soluble and is likely to precipitate in situ (source of the strong T_2

contrast), further aiding the stability of the complex *in vivo*. The clearance of the nano-scale precipitate is expected to be slow compared to small molecular chelates, as seen previously with S-Gal® [25]. In similar experiments with S-Gal® we previously noted intense contrast immediately after injection due to T_2 shortening, whereas after one hour, the contrast declined considerably, presumably due to clearance [25]. By comparison, the current experiments used only 8% the concentration of FAC and 20% as much substrate, yet achieved ~13% reduction in baseline relaxation times over 2 h in the same tumor types. This indicates better retention and higher *in vivo* sensitivity to C3-GD in tumors compared to S-Gal®. The lower dose of FAC needed to achieve detectable contrast suggests greater potential feasibility for systemic delivery of the substrate/FAC combination for assessment of *lacZ* gene expression *in vivo*, though this has not been tested.

By analogy, alternative sugar moieties could be used to develop substrates to report other enzymes such as glucoronidases and glucosidases. The ability to observe both T_1 and T_2 contrast adds considerably to the confidence of identifying β-gal activity. Otherwise tissue heterogeneity may mask contrast. We chose to deliver the reporter system intra-tumorally in this proof of principle study to separate the effect of delivery from the activity on the observed contrast. In its existing state, this system can be useful for pre-clinical investigations of development and improvement of novel gene-therapy approaches. For potential human use, the system will need to be refined to the point where even endogenous Fe (up-regulated in cancer and a target for chelation therapy) can provide sufficient contrast. While intra-tumoral injections are sub-optimal for human use, we note that all the recent studies on gene-therapy in the clinic have used intra-tumoral/intra-organ injection of the adenoviral vector [29]. Most β-gal reporters to date also have required direct intra-tumoral injection, but systemic administration would be advantageous and remains a goal.

Acknowledgments

This research was supported in part by the NIH National Cancer Institute (R21 CA120774, R21 CA132096) and the Southwestern Small Animal Imaging Research Program (SW-SAIRP), which is supported in part by U24 CA126608 and P30 CA142543. NMR experiments were performed at the Advanced Imaging Research Center, an NIH BTRP facility (P41RR02584).

References

1. Gilad AA, Winnard PT Jr, van Zijl PC, Bulte JW. Developing MR reporter genes: promises and pitfalls. NMR Biomed. 2007; 20(3):275–90. [PubMed: 17451181]
2. Contag CH, Ross BD. It's not just about anatomy: in vivo bioluminescence imaging as an eyepiece into biology. J Magn Reson Imaging. 2002; 16(4):378–87. [PubMed: 12353253]
3. Hoffman R. Green fluorescent protein imaging of tumour growth, metastasis, and angiogenesis in mouse models. Lancet Oncol. 2002; 3(9):546–56. [PubMed: 12217792]
4. Kruger A, Schirrmacher V, Khokha R. The bacterial lacZ gene: An important tool for metastasis research and evaluation of new cancer therapies. Cancer Metastasis Rev. 1999; 17:285–94. [PubMed: 10352882]
5. Braybrooke JP, Slade A, Deplanque G, Harrop R, Madhusudan S, Forster MD, et al. Phase I study of MetXia-P450 gene therapy and oral cyclophosphamide for patients with advanced breast cancer or melanoma. Clin Cancer Res. 2005; 11(4):1512–20. [PubMed: 15746054]
6. Eustice DC, Feldman PA, Colberg-Poley AM, Buckery RM, Neubauer RH. A sensitive method for the detection of beta-galactosidase in transfected mammalian cells. Biotechniques. 1991; 11(6):739–740. 742–733. [PubMed: 1809326]
7. Horwitz JP, Chua J, Curby RJ, Tomson AJ, Darooge MA, Fisher BE, et al. Substrates for cytochemical demonstration of enzyme activity. I. Some substituted 3-indolyl-beta-d-glycopyranosides. J Med Chem. 1964; 7:574–5. [PubMed: 14221156]

8. Heuermann K, Cosgrove J. S-Gal: an autoclavable dye for color selection of cloned DNA inserts. Biotechniques. 2001; 30(5):1142–7. [PubMed: 11355350]
9. Dimri GP, Lee X, Basile G, Acosta M, Scott G, Roskelley C, et al. A biomarker that identifies senescent human cells in culture and in aging skin in vivo. Proc Natl Acad Sci. 1995; 92(20):9363–7. [PubMed: 7568133]
10. Bandyopadhyay D, Gatza C, Donehower LA, Medrano EE. Analysis of cellular senescence in culture in vivo: the senescence-associated beta-galactosidase assay. Current protocols in cell biology / editorial board, Juan S Bonifacino [et al.]. 2005; Chapter 18(Unit 18 19)
11. Tung CH, Zeng Q, Shah K, Kim DE, Schellingerhout D, Weissleder R. In vivo imaging of beta-galactosidase activity using far red fluorescent switch. Cancer Res. 2004; 64(5):1579–83. [PubMed: 14996712]
12. Josserand V, Texier-Nogues I, Huber P, Favrot MC, Coll JL. Non-invasive in vivo optical imaging of the lacZ and luc gene expression in mice. Gene Ther. 2007; 14(22):1587–93. [PubMed: 17882264]
13. Liu L, Mason RP. Imaging beta-galactosidase activity in human tumor xenografts and transgenic mice using a chemiluminescent substrate. PLoS One. 2010; 5(8):e12024. [PubMed: 20700459]
14. Li L, Zemp RJ, Lungu G, Stoica G, Wang LHV. Photoacoustic imaging of lacZ gene expression in vivo. J Biomed Opt. 2007; 12(2):020504. [PubMed: 17477703]
15. Lee KH, Byun SS, Choi JH, Paik JY, Choe YS, Kim BT. Targeting of lacZ reporter gene expression with radioiodine-labelled phenylethyl-beta-D-thiogalactopyranoside. Eur J Nucl Med Mol Imaging. 2004; 31(3):433–8. [PubMed: 14745516]
16. Celen S, Deroose C, de Groot T, Chitneni SK, Gijsbers R, Debyser Z, et al. Synthesis and evaluation of 18 F- and 11C-labeled phenyl-galactopyranosides as potential probes for in vivo visualization of LacZ gene expression using positron emission tomography. Bioconjug Chem. 2008; 19(2):441–9. [PubMed: 18179161]
17. Louie AY, Huber MM, Ahrens ET, Rothbacher U, Moats R, Jacobs RE, et al. In vivo visualization of gene expression using magnetic resonance imaging. Nat Biotechnol. 2000; 18(3):321–5. [PubMed: 10700150]
18. Chang YT, Cheng CM, Su YZ, Lee WT, Hsu JS, Liu GC, et al. Synthesis and characterization of a new bioactivated paramagnetic gadolinium(III) complex [Gd(DOTA-FPG)(H2O)] for tracing gene expression. Bioconjug Chem. 2007; 18(6):1716–27. [PubMed: 17935289]
19. Yu JX, Kodibagkar VD, Hallac RR, Liu L, Mason RP. Dual (19)F/(1)H MR gene reporter molecules for in vivo detection of beta-galactosidase. Bioconjug Chem. 2012; 23(3):596–603. [PubMed: 22352428]
20. Cui W, Otten P, Li Y, Koeneman KS, Yu J, Mason RP. Novel NMR approach to assessing gene transfection: 4-fluoro-2-nitrophenyl-beta-D-galactopyranoside as a prototype reporter molecule for beta-galactosidase. Magn Reson Med. 2004; 51(3):616–20. [PubMed: 15004806]
21. Yu J, Otten P, Ma Z, Cui W, Liu L, Mason RP. Novel NMR platform for detecting gene transfection: synthesis and evaluation of fluorinated phenyl beta-D-galactosides with potential application for assessing LacZ gene expression. Bioconjug Chem. 2004; 15(6):1334–41. [PubMed: 15546200]
22. Yu JX, Ma Z, Li Y, Koeneman KS, Liu L, Mason RP. Synthesis and evaluation of a novel gene reporter molecule: detection of β-galactosidase activity using ^{19} F NMR of a fluorinated vitamin B6 conjugate. Med Chem. 2005; 1(3):255–62. [PubMed: 16787321]
23. Kodibagkar VD, Yu J, Liu L, Hetherington HP, Mason RP. Imaging beta-galactosidase activity using ^{19}F chemical shift imaging of LacZ gene-reporter molecule 2-fluoro-4-nitrophenol-beta-D-galactopyranoside. Magn Reson Imaging. 2006; 24(7):959–62. [PubMed: 16916713]
24. Yu JX, Kodibagkar VD, Liu L, Mason RP. A ^{19}F-NMR approach using reporter molecule pairs to assess beta-galactosidase in human xenograft tumors in vivo. NMR Biomed. 2008; 21(7):704–12. [PubMed: 18288788]
25. Cui W, Liu L, Kodibagkar VD, Mason RP. S-Gal®, A novel 1H MRI reporter for β-galactosidase. Magn Reson Med. 2010; 64(1):65–71. [PubMed: 20572145]
26. Yu JX, Gulaka PG, Liu L, Kodibagkar VD, Mason RP. Novel Fe^{3+} Based ^{1}H MRI β -galactosidase reporter molecules. Chem Plus Chem. 2012; 77:370–8. [PubMed: 23807909]

27. Liu ZD, Hider RC. Design of iron chelators with therapeutic application. Coord Chem Rev. 2002; 232(1–2):151–71.

28. Zhou T, Ma Y, Kong X, Hider RC. Design of iron chelators with therapeutic application. Dalton Trans. 2012; 41(21):6371–89. [PubMed: 22391807]

29. Duarte S, Carle G, Faneca H, de Lima MC, Pierrefite-Carle V. Suicide gene therapy in cancer: where do we stand now? Cancer Lett. 2012; 324(2):160–70. [PubMed: 22634584]

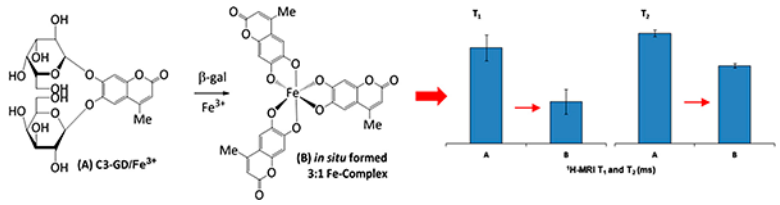

Fig. 1.
The illustration of mechanism for ^{1}H-MRI detection of β-gal activity, using C3-GD as a model reporter.

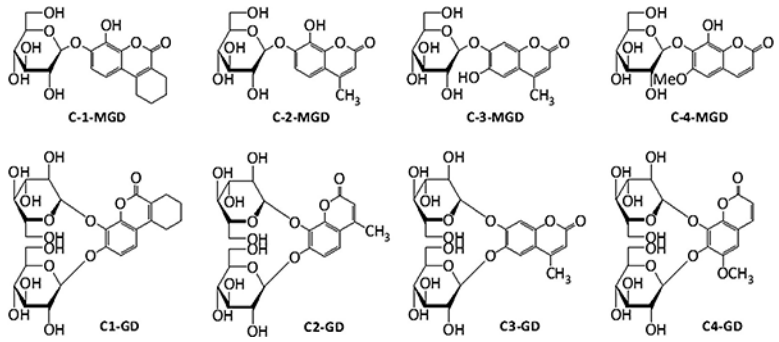

Fig. 2.
The structures of mono- and di-galactoside analogs of S-gal®.

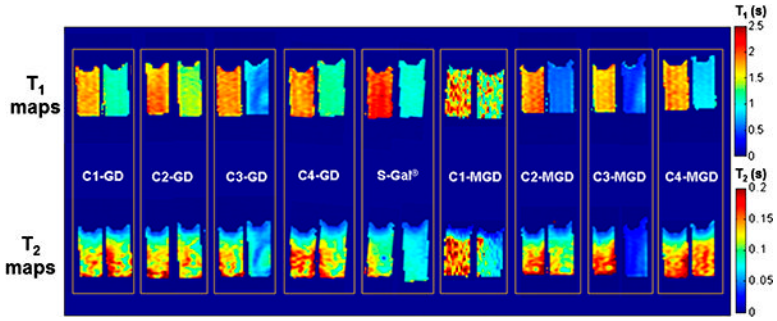

Fig. 3.

In vitro lacZ gene reporter activity of various analogs of S-gal ®. T_1 (top row) and T_2 (bottom row) maps of each sample containing 15 mM agent + 5 mM FAC in agarose without or with 5 units of β-gal enzyme (left and right sample in each box, respectively). Pronounced T_1 and T_2 effects are seen for the agents C3-GD and C3-MGD.

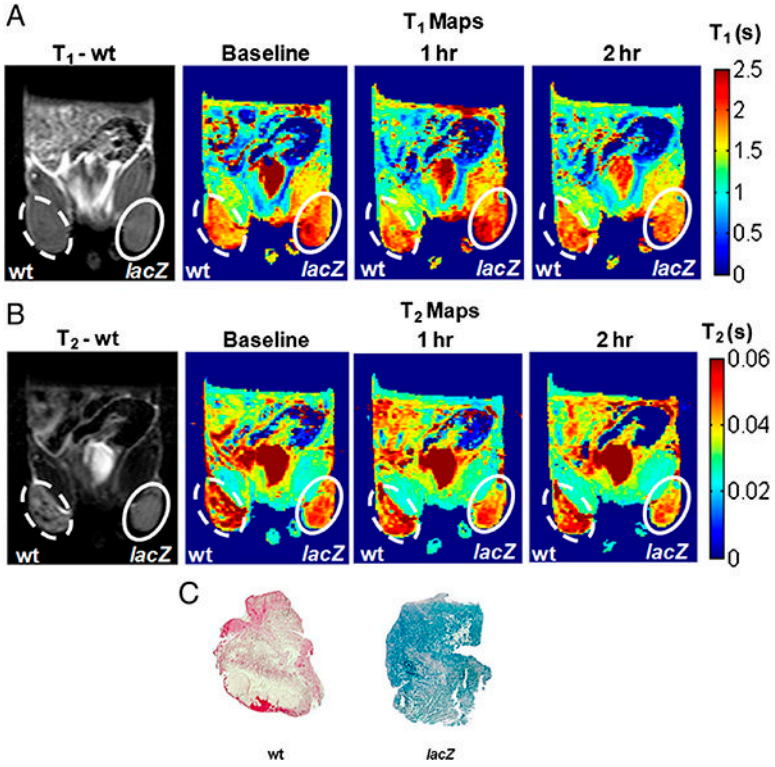

Fig. 4.

In vivo lacZ gene reporter activity of C3-GD. MRI of a representative nude mouse with wild type MCF7 tumor (left, dotted) and *lacZ* transfected MCF7 tumor (right, solid). A) Baseline T_1 weighted image and T_1 maps obtained before, 1 h after, and 2 h after direct intra tumoral injection of 15 mM C3-GD and 5 mM FAC (top row) and B) corresponding T_2 weighted images and T_2 maps (bottom row) showed decrease in the relaxation times in *lacZ* transfected tumors. C) X-gal and Nuclear fast staining of slices (whole mount) from the same wild type MCF7 (left) and MCF7-*lacZ* (right) tumors showed β-gal activity (intense blue stain from X-gal) for the MCF7-*lacZ* tumor section only.

Table 1

In vitro comparison of various analogs of S-gal® as MR gene reporter molecules: T_1 and T_2 (mean ± standard deviation) of the synthesized gene reporter molecules (7.5 mM) in the absence or presence of β-galactosidase (5 units) in 1% agar containing ferric ammonium citrate (FAC, 2.5 mM).

Agent	T_1 (s)		$\Delta R_1^{\beta-gal}$ (s^{-1})	T_2 (ms)		$\Delta R_2^{\beta-gal}$ (s-1)
	w/o β-gal	w/β-gal		w/o β-gal	w/β-gal	
C1-MGD	1.79 ± 0.28	1.46 ± 0.19	0.13	0.13 ± 0.04	0.09 ± 0.03	3.42
C2-MGD	1.83 ± 0.13	0.58 ± 0.05	1.18	0.12 ± 0.05	0.10 ± 0.03	1.72
C3-MGD	1.68 ± 0.12	0.51 ± 0.13	1.37	0.13 ± 0.05	0.03 ± 0.01	22.09
C4-MGD	1.78 ± 0.09	0.84 ± 0.05	0.63	0.13 ± 0.05	0.13 ± 0.03	0.09
S-Gal®	2.07 ± 0.12	1.04 ± 0.05	0.48	0.09 ± 0.03	0.07 ± 0.01	3.41
C1-GD	1.76 ± 0.13	1.11 ± 0.09	0.33	0.12 ± 0.03	0.12 ± 0.04	−0.84
C2-GD	1.81 ± 0.15	1.39 ± 0.09	0.17	0.12 ± 0.05	0.11 ± 0.03	0.76
C3-GD	1.83 ± 0.15	0.72 ± 0.12	0.84	0.11 ± 0.04	0.07 ± 0.01	5.97
C4-GD	1.85 ± 0.15	1.18 ± 0.06	0.31	0.13 ± 0.05	0.11 ± 0.04	1.67

Also listed are the corresponding differences in the relaxation rates due to β-galactosidase ($\Delta R_1^{\beta-gal}$ and $\Delta R_2^{\beta-gal}$, respectively). T_1 and T_2 values of the agents C3-GD and C3-MGD decreased the most in the presence of the enzyme.

Magn Reson Imaging. Author manuscript; available in PMC 2014 July 01.

Table 2

In vivo lacZ gene reporter activity of C3-GD: T_1 and T_2 (mean ± standard deviation) obtained from ROI analysis of *in vivo* data (n = 6) from wild type and *lacZ* transfected MCF7 tumors.

	T_1 (s)		$\Delta R_1^{\beta-gal}$	**T_2 (ms)**		$\Delta R_2^{\beta-gal}$
	MCF7-WT	**MCF7-*lacZ***	**(s^{-1})**	**MCF7-WT**	**MCF7-*lacZ***	**(s^{-1})**
Baseline	1.84 ± 0.28	1.88 ± 0.22	−0.01	56 ± 16	51 ± 8	1.75
1 hr post injection	1.72 ± 0.29*	1.69 ± 0.33*	0.01	51 ± 16*	44 ± 10*	3.12
2 hr post injection	1.97 ± 0.35*	1.63 ± 0.25*	0.51	57 ± 18	44 ± 9*	5.18
Change over 1 hr	−6.5%	−10.1%	-	−8.9%	−13.7%	-
Change over 2 hr	7.1%	−13.3%	-	1.7%	−13.7%	-

Also listed are the corresponding differences in the relaxation rates (between wild type and *lacZ* tumor) due to β-galactosidase ($\Delta R_1^{\beta\text{-gal}}$ and $\Delta R_2^{\beta\text{-gal}}$, respectively). MCF7-*lacZ* tumors showed a significant decrease in both T_1 and T_2 values at 2 h post injection compared to baseline.